Materials Today: Proceedings 46 (2021) 2612–2615

Contents lists available at ScienceDirect

Materials Today: Proceedings

journal homepage: www.elsevier.com/locate/matpr

High temperature corrosion behaviour of stainless steels and Inconel 625 in hydroxide salt

M. Pooja [a,*], K.S. Ravishankar [b], Vasudeva Madav [a]

[a] Department of Mechanical Engineering, National Institute of Technology Karnataka, Surathkal, Mangalore 575025, India
[b] Department of Metallurgical & Materials Engineering, National Institute of Technology Karnataka, Surathkal, Mangalore 575025, India

ARTICLE INFO

Article history:
Received 3 January 2021
Received in revised form 4 February 2021
Accepted 8 February 2021
Available online 18 March 2021

Keywords:
Molten salt
Intergranular corrosion
Corrosion rate
Weight loss
Spalling

ABSTRACT

Biomass gasification had proven to be an alternative source of energy to coal gasification. However, it requires high temperatures of about 1000°C for biomass drying and reduction. On the other hand, to reduce the oxidation and corrosion of gasifier structural materials it is important to keep the gasifier working temperature as low as possible. One effective way of keeping the reduction temperature low is to use molten salts as catalyst during biomass gasification. However, by virtue, molten salts cause several corrosion issues in ferrous alloys. In this context, the present study investigates the effect of hydroxide molten salt on the corrosion behaviour of stainless steels such as 316 and 310 and Inconel 625. The samples exposed to the salt at 700°C for about 48 h was analysed for corrosion using weight loss method. A scanning electron microscopy analysis of the exposed samples revealed the depth of corrosion and change in microstructure due to molten salt attack. Although all the selected materials suffered severe corrosion, among all, Inconel 625 show higher corrosion resistance.
© 2021 Elsevier Ltd. All rights reserved.
Selection and peer-review under responsibility of the scientific committee of the International Conference on Smart and Sustainable Developments in Materials, Manufacturing and Energy Engineering.

1. Introduction

The syngas and residues from gasification process have wide variety of applications, in power generation and chemical productions [1]. In principle, gasification is a combustion process, where the feedstock is (biomass) burnt with limited supply of air or oxygen to yield low/medium energy gases for power production [2]. The temperature of gasification may vary between 600°C and 1500°C depending on the gasifier type and its yield. Biomass gasification though proven to be an eternal source of energy, have presented several issues related to the supply and storage of the feedstock, their pre-treatment and waste disposal [3]. Additionally, the reducing atmosphere in gasification suppresses the formation of protective oxide layers in structural steels and accelerates corrosion. Presence of highly active elements such as Sulphur and chlorine in the gas form aggressive environments attacking the exposed materials in addition to the abrasive particles such as silica present in the hot gas. [4]. An alternative way to decrease high temperature corrosion in a gasifier is to employ an appropriate catalyst/molten salt that accelerates the gasification reaction and allows the reactions to take place at a lower temperature [5]. Though this retards the rate of corrosion due to operating temperatures, the use of inorganic salts in the process would react with the materials and boost corrosion. The inorganic molten salts act as a catalyst to improve the rate of reaction during biomass gasification. In the presence of inorganic salts, the syngas reaction will be formed at a much lower temperature as the salts act as a heat carrier. The catalyst enhances the gasification rate by about 3.3 times when compared to biomass with no molten salts [6]. Molten salts such as Flourides, Chlorides, Nitrates, hydroxides, carbonates and their eutectic mixtures are employable to improve the reaction rates and operating temperature of the salts vary from 120°C to 1000°C. However, the choice of the salts depends on the corrosive nature of the salts and corrosion resistance of the materials used in the reactor vessel and other allied process.

Although, the inorganic salts possess high heat capacity, thermal stability and catalytic properties, the severe corrosiveness of the salts demand highly corrosion resistance materials such as stainless steels and nickel super alloys in gasifiers [7]. However, in the presence of molten salts containing sulphur, the sulfidation

* Corresponding author.
E-mail addresses: poojamaithal@gmail.com (M. Pooja), vasu@nitk.edu.in (V. Madav).

https://doi.org/10.1016/j.matpr.2021.02.266
2214-7853/© 2021 Elsevier Ltd. All rights reserved.
Selection and peer-review under responsibility of the scientific committee of the International Conference on Smart and Sustainable Developments in Materials, Manufacturing and Energy Engineering.

Table 1
Composition of the substrate material.

Material/Element	C	Ni	Cr	Mn	Si	Mo	Fe	Nb	Al	Co
SS316	0.06	12	17	1.5	0.5	2.5	Bal	–	–	–
SS310	0.2	20	25	1.5	1	–	Bal	–	–	–
Inconel 625	0.07	65	22	0.5	0.5	9	4	4	0.4	1

Table 2
Specification of the samples (ASTM G162-18).

S.No	Material parameter	Material specification (mm)
1.	Length of the sample	40
2.	Width of the sample	30
3.	Thickness of the sample	5

of nickel and iron-based alloys would take place in the temperature range of 300 to 700°C, which results in the formation of Nickel sulphide, iron sulphide and chromium sulphide [8]. On the other hand, chlorine based salts results in the complex reactions of the steel with HCl, Cl_2, O_2 and H_2O and form of iron chlorides. The corrosion rate depends on the amount of chlorine in salt and the temperature of the exposure [9]. The nitrate salts are less corrosive than fluoride salts, however, due to their thermal instability, limited to low operating temperatures. Fernandez et al suggested alumina forming austenitic steel (AFA) for nitrate salt atmosphere. AFA showed excellent corrosion resistance by the formation of a highly protective Al-Cr rich oxide layer [10]. While, Dorcheh et al [11] studied the corrosion behaviour of low Cr steel, SS 316, SS374 and Inconel 625 in nitrate salts at 600°C. They observed that the nitrate exposure resulted in scale formation in stainless steel, while the Inconel developed a thick NiO layer. The exposure of Ni-Cr based alloys to nitrate salts resulted in the formation protective oxide Cr_2O_3 and NiO layers addition to the formation of iron oxide.

General surface corrosion with dissolution of Chromium oxide into melt takes place while Ni/Fe oxide remain insoluble. Li et al [12] reported that the exposure of Ni-Cr based alloys to fluoride salt would result in the inward diffusion of Ni and Cr and enhancement of corrosion. In a similar study, among the Ni-Cr alloys coated with Ni exposed to fluoride salt at 650°C in graphite crucibles, Ni-coated Hastealloy B performed better than other alloys [13]. Inconel 600 exposed to chloride salt at different operating temperatures ranging from 700 to 900°C for 100 h showed optimum corrosion resistance at about at 900°C due to the formation of a thick Cr_2O_3 protective layer. At 700°C, the alloy failed to produce a protective layer. The protective layer underwent dissolution, since the dissolution rate was higher than the growth rate [14]. In a recent study on carbon steel exposed to molten nitrate salt, two different forms of corrosion was evidenced, oxidation and carbonization at high temperature of 500°C [15]. A very high rate of corrosion was observed in plain carbon steel and inconel 600 when exposed to nitrate salt for about 2000 hrs [16]. In general, molten salts cause either leaching (dissolution) and/or intergranular attack in the exposed metals [17].

Differently, the present study investigates the effect of sodium hydroxide salt on the corrosion behaviour of different stainless steels and nickel alloy at high temperature. Past studies evidenced the formation of large amounts of H_2 and lesser carbon containing gases when NaOH was used in molten salt gasification [18]. Considering gasification temperature is between 800–900°C, the operating temperature of 700°C was used for the study, assuming that the gasification reactions proceed at lower temperatures in the presence of molten salts. The conventional weight loss method was used for corrosion testing, SEM, and EDAX for characterization.

2. Experimental methodology

2.1. Material and specification

Three-substrate material (Stainless steel grades 316, 310 and Inconel 625) was chosen for the study, the chemical composition of the substrates is shown in Table 1. The dimensions of the samples used for corrosion tests as per standard ASTM are given in Table 2.

2.2. Corrosion studies

To study the hot corrosion behaviour of steels and nickel-based alloy, samples were exposed to high temperature muffle furnace containing molten salts. The schematic representation of the exposed sample in furnace is shown in Fig. 1. The samples for study were cut to standard dimensions 40 × 30 × 5 mm by laser cutting for precision. The specimen was polished on all the sides by standard metallographic techniques prior exposure. A 2 mm hole was drilled on the top of the specimen to suspend it into the furnace. A steel wire of 0.5 mm diameter was used for suspension. The salt was placed inside the furnace in a stainless-steel container after the furnace temperature reaches a desired value. The temperature inside the container was adjusted by means of a thermocouple. After the molten salts attain the desired temperature, the samples were exposed and placed for a definite exposure period. The samples after exposure was cooled to room temperature. Acetone was used for washing and the samples then dried. The samples were cut along the cross section to study the corrosion products and the oxide layer. Various characterisation techniques mentioned in previous sections was used for analysis of the specimen.

2.3. Weight loss investigation

The weight of the samples before and after exposure is measured. Assuming uniform corrosion all over the specimen, the corrosion rate in millimetre per year by weight loss method can be determined using the relation,

$$CR = W/(D \times A \times t) \times k(87.6)$$

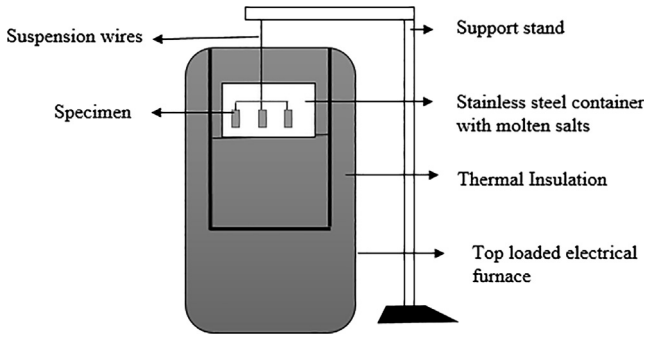

Fig. 1. Schematic of the specimen exposed in furnace in molten salts.

Table 3
Corrosion rates of samples in mpy.

Sl.No	Material	Density g/cm^3	Initial weight in grams	Final weight	Weight loss in grams	Corrosion rate	
						In mm/y	In mpy
1.	SS316	8	45.47	43.9592	1.5108	11.1	438
2.	SS310	8	43.3075	42.063	1.2445	9.1	359
3.	Inconel 625	8.44	62.65	61.98	0.67	4.93	194

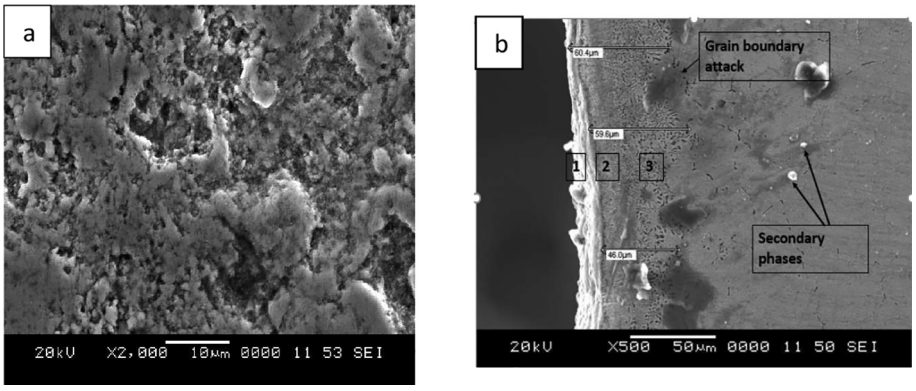

Fig. 2. (a) Surface morphology of 310SS after 48 hrs exposure. (b) Oxide layers formed.

where CR – Corrosion rate in mm/y, W – Weight loss in milligrams, D – Density of the sample in g/cm^3, A – Area of the sample in cm^2, t – Exposure period in hours.

2.4. Microstructural characterisation

The exposed samples were cleaned using acetone and then dried. The thick oxide scale was removed by belt grinding. The surface morphology was obtained using 100, 200, 300, 400 grit silicon carbide papers, followed by cloth polishing with alumina. The sample was then dried and etched with aqua regia. Micro structural characterisation comprises of study under Optical and Scanning electron microscopy to determine the presence and extent of growth of oxide layer and interdiffusion of any species through EDAX. Scanning electron microscope equipped Electron back scattered detector (EBSD) and Energy dispersive spectroscopy (EDS) was used in this study. Scanning electron microscope equipped Electron Back Scattered Detector (EBSD) and Energy Dispersive Spectroscopy (EDS) was used in this study. EDS was used to measure the chemical composition of a point in the microstructure. SEM image was used to study corrosion morphology. The study of coating thickness, growth of oxide film, the interdiffusion of any species and the extent of diffusion is performed using SEM.

3. Results and discussions

The corrosion rates of the tested specimens is shown in the Table 3. From the table, it can be inferred that all the samples underwent extensive corrosion when exposed to sodium hydroxide salt at high temperature. However, the resistance to corrosion is higher in nickel alloy was comparatively better than the stainless steel alloys. This may be due to the high nickel content in Inconel 625.

The surface morphology of 310SS after 48 h exposure in sodium hydroxide salt at 700°C is shown in Fig. 2a. The upper surface indicated a layer of semi-continuous oxidation product. Fig. 2b shows the cross section of 310SS indicating three distinct oxide layers. It is evident from the EDS analysis that these are Ni/Fe/Cr oxide layers. The outermost layer is a Cr rich protective oxide deposit, whereas inner regions are Cr depleted and Fe rich, hence accelerated IGC. High temperature exposure intiated initiated microstructural changes in the sample, increasing its susceptibility to intergranular corrosion. This type of corrosion results in the reduction of strength of the metal at regions where the cracks has propogated. In addition, the formation of secondary phases may accelerate corrosion, by acting as nucleation sites IGC. Fig. 3a shows the surface morphology of 316SS exposed to hydroxide salt

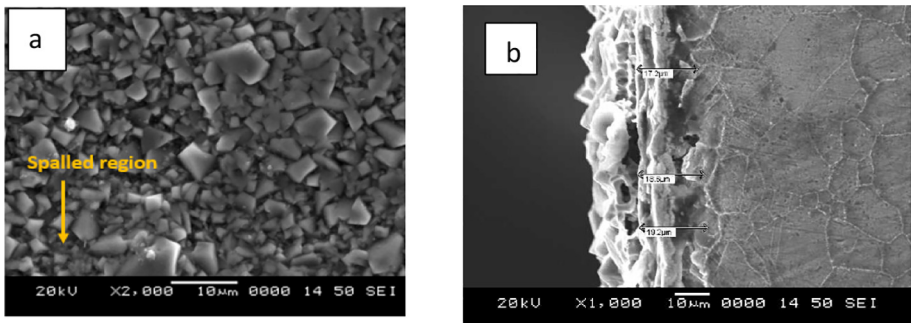

Fig. 3. (a) Surface morphology of 316SS after 48 hrs exposure. (b) Oxide layer formed.

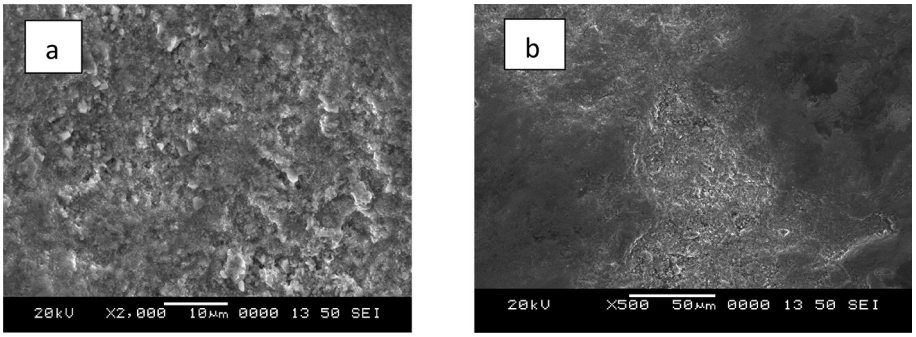

Fig. 4. (a) Surface morphology of Inconel 625 after 48 hrs exposure. (b) Oxide layers formed.

at 700°C for 48 hrs. It is important to note the spalling behaviour with a large number of oxide islets in the spalled region. From literature, this is evident that these are Cr rich structures while the irregular granular constitution in the unspalled region constitute Fe rich fine oxide particles.

Fig. 3b shows the surface SEM images of 316SS. It is found that the oxide scale is loosely adhered to the surface and is porous. In addition, very severe grain peeling off is evident at the boundary near the oxide layer. The intergranular corrosion has penetrated deep into the metal and the grains have peeled off from the base metal. It is revealed that the intergranular corrosion is more severe in 316SS when compared to 310SS. The extent of grain peeling-off is more critical in 316SS. Fig. 4a shows the surface morphology of Inconel 625 exposed to sodium hydroxide salt at 700°C for 48 hrs. The SEM and EDS analysis shows the presence of two distinct oxide layers; an outer loose compact layer and an inner fine grained oxide layer. The outer non-protective layer is the NiO while the inner layer is a protective layer of Cr_2O_3. This is attributed to large Cr content in the alloy i.e. greater than 14%, which is the major criteria for the formation of Cr rich oxide layer.

4. Conclusions

- Both grades of stainless steels, 310SS and 316SS underwent severe corrosion by intergranular attack. The susceptibility is higher in 316SS leading to a large number of grainpeeling off from the base metal.
- The sodium hydroxide salt causes severe corrosion in both stainless steel and Inconel 625. However. Inconel 625 has better corrosion resistance as compared to SS.

CRediT authorship contribution statement

M. Pooja: Conceptualization, Methodology, Data curation, Writing - original draft. **K.S. Ravishankar:** Supervision, Writing - review & editing. **Vasudeva Madav:** Supervision, Writing - review & editing.

Declaration of Competing Interest

The authors declare that they have no known competing financial interests or personal relationships that could have appeared to influence the work reported in this paper.

References

[1] J.P. Bennett, K.-S. Kwong, Failure mechanisms in high chrome oxide gasifier efractories, Metall. Mater. Trans. A 42 (4) (2011) 888–904.
[2] T.B. Reed. 1979. Survey of biomass gasification, volume II: principles of gasification. NREL/TR-33-239, 5901867.
[3] R.W. Breault, Gasification processes old and new: a basic review of the major technologies, Energies 3 (2) (2010) 216–240.
[4] J. Tylczak. 2004. High Temperature Erosion Testing in a Gasifier Environment. 16.
[5] B.J. Hathaway, D.B. Kittelson, J.H. Davidson, Development of a molten salt reactor for solar gasification of biomass, Energy Procedia 49 (2014) 1950–1959.
[6] H.S. Nygård, E. Olsen, Review of thermal processing of biomass and waste in molten salts for production of renewable fuels and chemicals, Int. J. Low-Carbon Technol. 7 (4) (2012) 318–324.
[7] S. Heidenreich, M. Müller, P.U. Foscolo. 2016. Chapter 4 – Advanced Process Integration: The Unique Gasifier Concept—Integrated Gasification, Gas Cleaning and Conditioning. Adv. Biomass Gasif.. Academic Press. 18–54.
[8] N.S. Patel, V. Pavlík, M. Boča, High-temperature corrosion behavior of superalloys in molten salts – a review, Crit. Rev. Solid State Mater. Sci. 42 (1) (2017) 83–97.
[9] A. Soleimani Dorcheh, R.N. Durham, M.C. Galetz, Corrosion behavior of stainless and low-chromium steels and IN625 in molten nitrate salts at 600°C, Sol. Energy Mater. Sol. Cells 144 (2016) 109–116.
[10] A.G. Fernández, A. Rey, I. Lasanta, S. Mato, M.P. Brady, F.J. Pérez, Corrosion of alumina-forming austenitic steel in molten nitrate salts by gravimetric analysis and impedance spectroscopy: corrosion in molten nitrate salts, Mater. Corros. 65 (3) (2014) 267–275.
[11] X. Li, S. He, X. Zhou, P. Huai, Z. Li, A. Li, X. Yu, High-temperature corrosion behavior of Ni–16Mo–7Cr–4Fe superalloy containing yttrium in molten LiF–NaF–KF salt, J. Nucl. Mater. 464 (2015) 342–345.
[12] W.-J. Cheng, R.S. Sellers, M.H. Anderson, K. Sridharan, C.-J. Wang, T.R. Allen, Zirconium effect on the corrosion behavior of 316L stainless steel alloy and hastelloy-N superalloy in molten fluoride salt, Nucl. Technol. 183 (2) (2013) 248–259.
[13] S.S. Sawant, B.D. Gajbhiye, S. Tyagi, C.S. Sona, R. Divya, C.S. Mathpati, A. Borgohain, N.K. Maheshwari, High temperature corrosion studies in molten salt using salt purification and alloy coating, Indian Chem. Eng. 59 (3) (2017) 242–257.
[14] G. Salinas-Solano, J. Porcayo-Calderon, J.G. Gonzalez-Rodriguez, V.M. Salinas-Bravo, J.A. Ascencio-Gutierrez, L. Martinez-Gomez, High temperature corrosion of inconel 600 in NaCl-KCl molten salts, Adv. Mater. Sci. Eng. (2014) 1–8.
[15] Y. Grosu, U. Nithiyanantham, A. Zaki, et al., A simple method for the inhibition of the corrosion of carbon steel by molten nitrate salt for thermal storage in concentrating solar power applications, npj Mater. Degrad. 2 (2018) 34.
[16] Sequeira, César. 2019. High Temperature Corrosion: Fundamentals and Engineering. Chapter 9. 296–324. 10.1002/9781119474371.
[17] A. Palacios, M.E. Navarro, Z.u. Jiang, A. Avila, G. Qiao, E. Mura, Y. Ding, High-temperature corrosion behaviour of metal alloys in commercial molten salts, Solar energy 201 (2020) 437–452.
[18] A.B. Koven, S.S. Tong, R.R. Farnood, et al., Alkali thermal gasification and hydrogen generation potential of biomass, Front. Chem. Sci. Eng. 11 (2017) 369–378.